Development 130, 3427-3436

doi:10.1242/dev.00569

Monitoring neural progenitor fate through multiple rounds of division in an intact vertebrate brain

David A. Lyons, Adam T. Guy and Jonathan D. W. Clarke*

Centre for Cellular and Molecular Dynamics, Department of Anatomy and Developmental Biology, University College London, Gower Street, London WC1E 6BT, UK

*Author for correspondence (e-mail: jonathan.clarke@ucl.ac.uk)

Accepted 25 April 2003

SUMMARY

The behaviour of neural progenitors in the intact vertebrate brain and spinal cord is poorly understood, chiefly because of the inaccessibility and poor optical qualities inherent in many model systems. To overcome these problems we have studied the optically superior brain of the zebrafish embryo and have monitored the in vivo behaviour of fluorescently labelled neural progenitors and their daughter cells throughout a substantial period of hindbrain development. We find the majority (84%) of hindbrain neurons are born from progenitor divisions that generate two neurons and 68% of reconstructed lineage trees contained no asymmetric stem cell-like divisions. No progenitors divided in the manner expected of a classic stem cell; i.e. one that repeatedly self-renews and generates a differentiated cell type by asymmetric division. We also analysed the orientation of progenitor divisions relative to the plane of the ventricular zone (VZ) and find that this does not correlate with the fate of the daughter cells. Our results suggest that in this vertebrate system the molecular determinants that control whether a cell will become a neuron are usually not linked to a mechanism that generates asymmetric divisions.

Key words: In vivo imaging, Vertebrate neurogenesis, Neural progenitor cell fate, Asymmetric division, Zebrafish

INTRODUCTION

During development of the vertebrate central nervous system (CNS), neurons are generated from the progenitor cells that lie within the ventricular zone (VZ) of the early neural tube. Although we have a broad understanding of how these progenitor cells behave as a population to generate neurons and glia, we know rather little about the behaviour of individual cells. For instance, it seems clear that progenitors must first undergo rounds of multiplicative division in order to increase the population of progenitor cells. This growth phase is followed by progenitor divisions that begin to generate neurons, and this could be accomplished by asymmetric divisions that generate both a neuron and another mitotically active progenitor or by divisions that generate two neurons. Clonal analyses in mammals and birds (e.g. Kornack and Rakic 1995; Mione et al., 1997; Lumsden et al., 1994; Reid et al., 1997; Noctor et al., 2001) suggest that both types of division are used during neurogenesis, but it is not clear which of these modes of division predominates or how they are co-ordinated over time. Throughout much of the period of vertebrate neurogenesis both growth and differentiation occur simultaneously and a balance between population growth and differentiation of some cells must be achieved.

Progenitor behaviour is better understood in invertebrate nervous systems and here asymmetric cell division appears to be a fundamental mechanism for generating cell diversity. In these systems asymmetric division is often based on the unequal partitioning of cytoplasmic determinants during division (reviewed by Lu et al., 2000) and this relies on mechanisms that co-ordinate the plane of progenitor division with the sub-cellular localisation of fate determinants. In *Drosophila* the neuroblast division is clearly asymmetric in that cytoplasmic determinants are inherited asymmetrically by daughter cells and daughter cells have different fates (Hirata et al., 1995). However, the neuroblast division generates two progenitors, whereas in vertebrate studies an asymmetric division is typically defined as one that generates a progenitor and a neuron (e.g. Mione et al., 1997; Noctor et al., 2001; Cai et al., 2002). There are also clear cases in *Drosophila* in which an asymmetric division generates two daughter neurons that have different phenotypes (Bossing et al., 1996). In vertebrates the analysis of sister cell phenotypes in vivo has been very limited, but clonal analysis in the chick has provided evidence that individual progenitors often give rise to clones of neurons of a single subclass (Lumsden et al., 1994; Clarke et al., 1998), suggesting that in this system sister cells may become symmetrically fated neurons in vivo. The role that cytoplasmic determinants may play in asymmetric fate decisions in the vertebrate nervous system is not certain, but at least some aspects of the molecular machinery are conserved (e.g. Kubu et al., 2002; Petersen et al., 2002; Shen et al., 2002; Verdi et al., 1999; Wakamatsu et al., 1999; Wakamatsu et al., 2000; Zhong et al., 1997; Zhong et al., 2000; Zilian et al., 2001) and

orientation of division has been correlated with asymmetric cell behaviours in some vertebrate systems (Chenn and McConnell, 1995; Cayouette et al., 2001).

Many invertebrate neural progenitors undergo stereotyped, invariant patterns of division (e.g. Skeath and Doe, 1996; Brewster and Bodmer, 1996; Shankland, 1995). Whether invariant lineages occur in the vertebrate nervous system is not yet known. However, when progenitors of the cerebral cortex are dissociated from the early embryonic brain and cultured at low density, they can undergo a series of stereotyped cell divisions and fate decisions to generate a family of differentiated cell types (Qian et al., 1998). Furthermore, the normal sequence of neurogenesis followed by gliogenesis is maintained by cortical progenitors in culture (Qian et al., 2000). These results suggests that some progenitor cells could be programmed to generate invariant lineage trees, but whether such stereotyped patterns of division occur in the normal environment of the vertebrate brain is not certain.

Our understanding of the importance of asymmetric divisions and invariant lineage in the vertebrate brain is largely limited by its complexity, inaccessibility during the period of neurogenesis and its poor optical qualities. Here we use the relative simplicity, accessibility and superior transparency of the zebrafish CNS to overcome these difficulties. We have been able to follow the fate of neural progenitors through multiple rounds of cell division, covering a substantial period of zebrafish neurogenesis, reconstruct lineage trees and document the type of divisions that lead to neuronal birth.

MATERIALS AND METHODS

Embryo care

All embryos were staged according to Kimmel et al. (Kimmel et al., 1995). To inhibit pigmentation embryos were transferred to a solution of embryo medium containing 0.02 mM phenlythiocarmamide (PTU, Sigma) at 24 hours post-fertilisation (hpf).

BrdU labelling

BrdU (Sigma) was applied by pulse labelling in solution. Embryos were placed in a solution of 2 mg/ml BrdU in embryo medium with 15% DMSO for 20-30 minutes on ice. Embryos were left to recover at 28.5°C for at least 15 minutes afterwards.

HuC-GFP is pan-neuronal and expressed in neurons soon after birth

HuC is an RNA-binding protein thought to be expressed exclusively in neurons (Park et al., 2000a), and we have used the HuC-GFP transgenic line (Park et al., 2000b) in several of our analyses. In order to be sure that HuC-GFP was expressed only in post-mitotic cells, we labelled embryos with single pulses of BrdU at 24, 36, 60 and 72 hpf and checked for co-expression with HuC-GFP 30 minutes later. HuC-GFP cells were never BrdU-positive. We also determined how soon neurons expressed HuC-GFP after their birth. First we determined that 3 hours was the shortest time interval between BrdU pulses at 24 or 36 hpf and co-expression of the cell-cycle marker phosphohistone H-3 that marks the G2/M transition (Juan et al., 1998). We then determined that the shortest interval between BrdU pulse and HuC-GFP expression was 7 hours and were thus able to calculate the shortest interval between G2/M transition and HuC-GFP expression at these times. At both 24 and 36 hpf, HuC-GFP expression can be observed just 4 hours after G2/M transition. Considering that mitosis lasts approximately 1 hour and transcription and translation of HuC-GFP will take approximately 1-2 hours, we consider that HuC-GFP expression is a very early marker of neuronal differentiation.

Cell counting

Embryos were stained by placing them in 5 μM Bodipy 505/515, (Molecular Probes), or 5 μM Texas Red Bodipy Ceramide (Molecular Probes). Total cell numbers were counted from confocal z-series of living embryos stained with Bodipy 505/515, which outlines all cells. Counts were made from rhombomeres 4 and 5, which are largely lineage-restricted compartments (Fraser et al., 1990). The total number of non-neuronal cells was counted as HuC-GFP-negative cells in transgenic specimens counter-stained with Texas Red Bodipy ceramide. Total neuronal number was then calculated by subtracting these two numbers. The interval in the z plane was always smaller than the smallest unit to be counted, typically 3 μm. The unbiased disector method was used to count cells (Sterio, 1984) and was performed using NIH image. Volume estimation was performed using Volocity software (Improvision).

Cell-cycle length

In order to be confident of our lineage data, we wanted to estimate the number of cell cycles we could expect the labelled progenitors to complete within our observation period, so we have estimated the cell-cycle length at 36 hpf. First, using repetitive pulses of BrdU, we determined that BrdU needs to be present for at least 6 hours in order for incorporation into all progenitors. This suggests that the G2+M+G1 interval between S-phases is approximately 6 hours. Second, we determined that a single BrdU pulse at 36 hpf is incorporated into 42.5% of the total progenitor population, thus suggesting that S-phase occupies 42.5% of the cell cycle. Combining these data gives a minimum length of the cell cycle of 14 hours at 36 hpf. Thus, if the interval between observations is less than 14 hours, no cell should undergo more than one division in this time.

Single cell injection

Single cells were injected with fluorescent dextran in the region of neural plate or neural keel fated to generate rhombomeres 3-7 of the hindbrain. Cells in wild-type and HuC-GFP-positive embryos were labelled with a mixture of 1% Rhodamine Dextran (3000 MW, Molecular Probes) and 2% biotinylated dextran (Molecular Probes) by iontophoresis (see Clarke, 1999). To facilitate passing the electrode through the skin, embryos older than 9 hpf were incubated in a solution of 5 mg/ml pronase (Sigma), for one minute. Embryos were returned to embryo medium and were stabilised for iontophoresis by being placed on a drop of 2% methyl cellulose. Each specimen was examined after 10-20 minutes to ensure that only one healthy cell was labelled. Cells were re-observed every 8-12 hours. At each observation point, the number of cells, their morphology and their location were noted and cells were imaged from both dorsal and lateral aspects if necessary.

Imaging

Live and fixed embryos were imaged on either a Leica confocal microscope or a Zeiss Axioplan 2 fitted with a Hamamatsu Orca ER digital camera. Data was collected using either Leica confocal or Openlab software (Improvision). Deconvolution of z-stacks gathered on the Axioplan was performed using Openlab software. 3D analysis of confocal stacks was performed using either NIH image or Volocity (Improvision).

Immunochemistry

The following primary antibodies were used during this study. Mouse monoclonal anti-zrf-1 (1/4, Oregon Monoclonal bank), rabbit polyclonal anti-GFAP (1/100, kind gift of John Scholes), mouse monoclonal anti-acetylated tubulin (1/1000, Sigma), mouse monoclonal anti-BrdU (1/200, Sigma), rabbit polyclonal anti-GFP (1/1000, Torrey Pines Biolabs) and anti-phosphohistone H-3 (1/1000,

Upstate Biotechnology). The following secondary antibodies were used: Alexa 488 and 568 goat anti-mouse IgG and goat anti-rabbit IgG (Molecular Probes) and peroxidase-conjugated goat anti-mouse IgG (Sigma). All secondary antibodies were used at a concentration of 1/200. Texas Red Avidin (1/200, Zymed) was used to visualise cells injected with biotinylated dextran.

α-tubulin Gal4UAS-GFP DNA

α-tubulin Gal4UAS-GFP DNA (Koster and Fraser, 2001) was injected into the cytoplasm at the one-cell stage at a concentration of 20 ng/μl to generate embryos with a mosaically labelled nervous system. The GFP translated using this construct was excluded from the nucleus, which facilitated detailed imaging of cell morphology.

Acridine orange

The vital dye acridine orange [acridinium chloride hemi-(zinc chloride) (Sigma)] was used to detect apoptotic corpses in live embryos. Embryos were incubated in a solution at 5 μg/ml for 30 minutes and washed in embryo medium several times before imaging.

RESULTS

The majority of hindbrain neurons are born before 48 hpf

We have used the HuC-GFP transgenic line (Park et al., 2000b) to quantify hindbrain neurogenesis and in many of our lineage analyses. In this line, GFP is expressed in all neurons and we estimate that it takes as little as 4 hours to detect GFP fluorescence after neuronal birth (see Materials and Methods). The distribution of HuC-GFP cells and the development of the hindbrain neuroepithelium is illustrated in transverse sections in Fig. 1A-D. HuC-GFP is expressed in all neuronal processes as well as their cell bodies, thus the marginal zone as well as the mantle layer is brightly fluorescent. The VZ is apparent as a fluorescence-free zone and in the hindbrain assumes a characteristic T-shaped configuration by 36 hpf. By 48 hpf the mantle zone has a depth of approximately 10-12 cell diameters and this increases to approximately 14-16 cell diameters by 72 hpf.

To ensure that our studies cover the major period of hindbrain neurogenesis and account quantitatively for the numbers of neurons actually generated, we counted the total neuron and non-neuronal cell numbers in two hindbrain segments up to 72 hours of development (Fig. 1E,F). At 15 hpf, rhombomeres 4 and 5 together contain on average only 21 HuC-GFP-positive cells, and this rises to 300 at 24 hpf. Over the next 12 hours the rate of neurogenesis triples to make a total of 1407 neurons in r4 and r5 by 36 hpf. The rate increases again until 48 hpf when these segments contain 4150 neurons. The rate of neurogenesis then declines over the next 12 hours to make a total of 5607 neurons by 60 hpf. The number of neurons then remains approximately the same up to 72 hpf. The smooth curve of the graph suggests that hindbrain neurogenesis is a continuous process, not obviously divided into periods of primary and secondary neurogenesis (Fig. 1F). By 72 hpf the non-neuronal cells represent only 3% of the total cell population.

Individual progenitors can be followed through several rounds of division to their terminal mitosis

In order to analyse the generation of neurons, we have labelled single neural progenitors with fluorescent dextran and followed their fate over a large period of embryogenesis. Each labelled progenitor was checked at the time of injection to ensure that only one cell was labelled and then re-observed every 8-12 hours until the embryo was 48-72-hours old (Figs 2-4). The 8-12-hour interval is sufficient for only one round of division (see Materials and Methods). Most of our lineage analyses (54/86) were performed in the HuC-GFP line, thus eliminating the need to phenotype cells by morphology alone. We present our lineage tree analyses from a starting point of approximately 15 hpf when the hindbrain is at the neural rod stage of

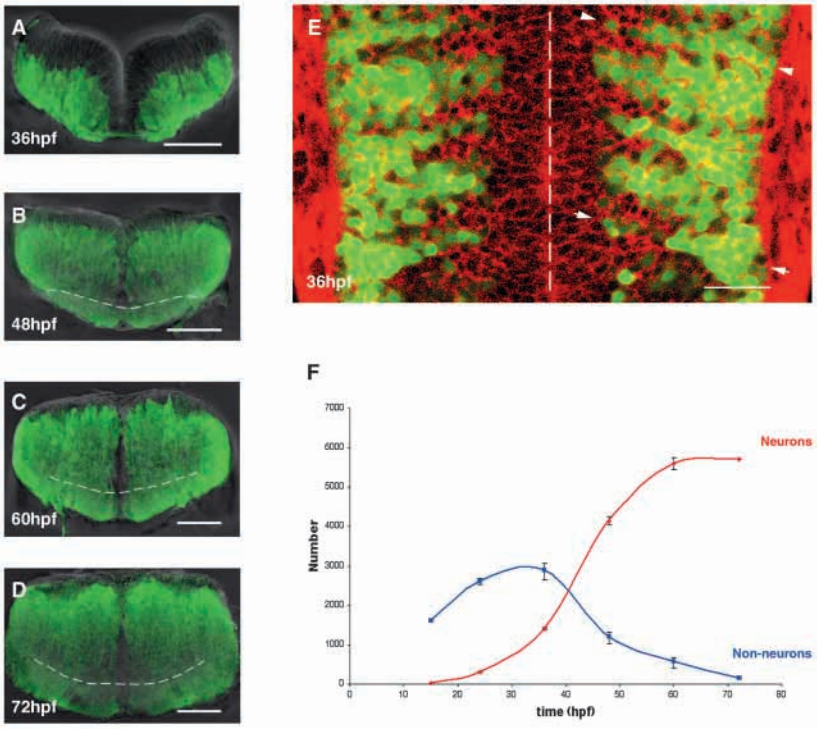

Fig. 1. Dynamics of hindbrain neurogenesis. (A-D) Transverse sections through the hindbrain at the level of rhombomeres 4 and 5 in HuC-GFP-positive embryos. The GFP fills both neuronal cell bodies and processes. Broken lines in B-D indicate the boundary between the mantle zone and the marginal zone. A distinct T-shaped ventricular zone is obvious at 36 hpf as an area devoid of HuC-GFP expression and this decreases dramatically by 48 hpf. Dorsal is to the top. (E) Horizontal confocal section through a living HuC-GFP-positive embryo stained with Texas Red Bodipy Ceramide to outline cell profiles. Arrowheads indicate the boundary between rhombomeres 3 and 4 and arrows indicate the boundary between rhombomeres 5 and 6. The embryonic midline is highlighted by a broken line. (F) Graph documenting numbers of neurons and non-neurons in rhombomeres 4 and 5 throughout embryogenesis. The red curve highlights the increase in neurons and the blue curve indicates the number of non-neuronal cells. Scale bars: 50 μm.

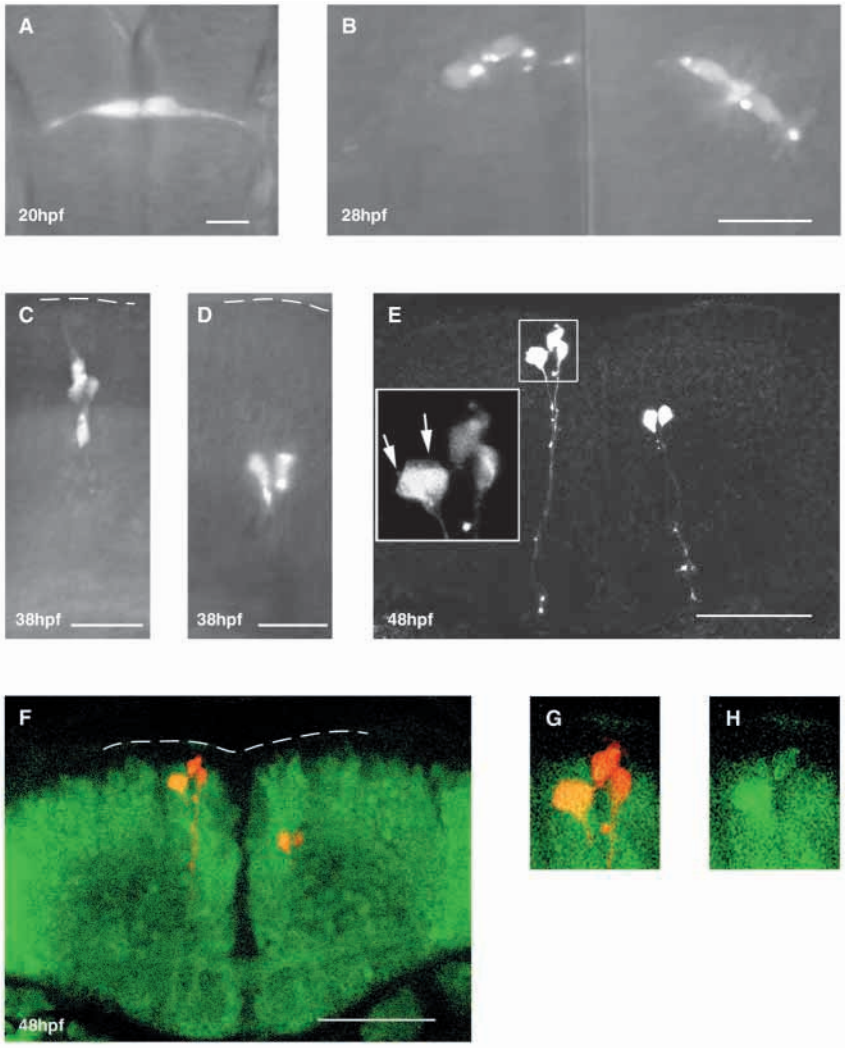

Fig. 2. Observations of two clones expanding throughout embryogenesis. (A) Dorsal view of an embryo at 20 hpf. Two elongated progenitor cells are seen, one on each side of the embryonic midline. Scale bar: 20 μm. (B) Dorsal view of the same specimen at 28 hpf. Both cells have divided. On the left-hand side daughter cells remain close to the ventricular zone, whereas on the other side two cells are seen further from the ventricular surface, suggesting they will become neurons. Scale bar: 20 μm. (C) Lateral view of cells on the left-hand side of the midline at 38 hpf. Four cells are now visible, suggesting that both cells seen at 28 hpf divided once more. The ventricular surface is indicated by a broken line. Scale bar: 20 μm. (D) Lateral view of cells on the right-hand side of the midline at 38 hpf. These two cells have moved further from the ventricular zone, indicating a neuronal phenotype. The ventricular surface is indicated by a broken line. Scale bar: 20 μm. (E) Confocal projection of the specimen fixed at 48 hpf. There are four cells (see inset) on the left side of the embryonic midline and two on the right, showing that none of the cells observed at 38 hpf divided. Transverse section with dorsal to the top. Scale bar: 50 μm. Arrows in inset indicate two cell bodies very close together. (F) Same section as in E but revealing underlying HuC-GFP expression. All dextran-labelled cells express HuC-GFP, indicating they are neurons. The ventricular surface is indicated by a broken line. Scale bar: 50 μm. (G) Magnified image of four cells on the left side of the midline showing all four co-express HuC-GFP and dextran. (H) Same image as in G showing the GFP channel alone.

development. Prior to this the cells of the neural plate have converged on the dorsal midline and most have undergone a single midline division that deposits one progenitor on either side of the neural midline (Kimmel et al., 1994) (Fig. 2A). We have monitored the development of 86 progenitors. The majority of these progenitors (79/86) resulted in clones containing only neurons, and for each of these clones we have successfully reconstructed their lineage tree. The remaining 7/86 progenitors generated clones containing a mixture of neurons and radial cells (putative progenitors) at the end of their analysis. We will describe the analyses of these two classes of clones separately.

Development of neuron-only clones

From the 79 neuron-only clones we have monitored the ancestry of 222 neurons. Early in clonal expansion cells have typical progenitor morphology (Fig. 2A,B) and at later time-points cells are found further away from the ventricular surface (Fig. 2C) and lose their ventricular connections (Fig. 2D). Having moved away from the VZ, cells then express HuC-GFP (Fig. 2F-H, Fig. 3B,E) and within the mantle layer are often seen to possess axon-like processes and growth cones (Fig. 3C-E, Fig. 4).

The range of lineage trees that were characterised in their entirety is shown in Fig. 5A. The reconstructed trees for neuron-only clones fall into two clear categories. Most trees (46/68 or 68%) contain no divisions that generated a neuron and a further progenitor, whereas in the remainder (22/68 or 32%) one or two such asymmetric divisions are seen (Fig. 4, Fig. 5A). When present, these asymmetric divisions were usually the first division of the lineage (19/22) and usually one cell-cycle before the terminal divisions of that tree, thus generating a three neuron sub-clone motif (19/22) (see Fig. 4 and Fig. 5A). None of the fully reconstructed lineage trees contain a progenitor that follows a classic stem-cell mode of division; i.e. one that self-renews and generates a differentiated cell-type at each division. The clones were evenly distributed in the mantle layer of the hindbrain (Fig. 5B), suggesting that we have sampled progenitors from many regions of the VZ.

Most neurogenic divisions generate a pair of neurons

Of the 222 neurons observed, the large majority (186/222 or 84%) were born from progenitor divisions that generated a pair of neurons and only 25/222 (11%) were born from asymmetric divisions that generated a neuron and a progenitor. The

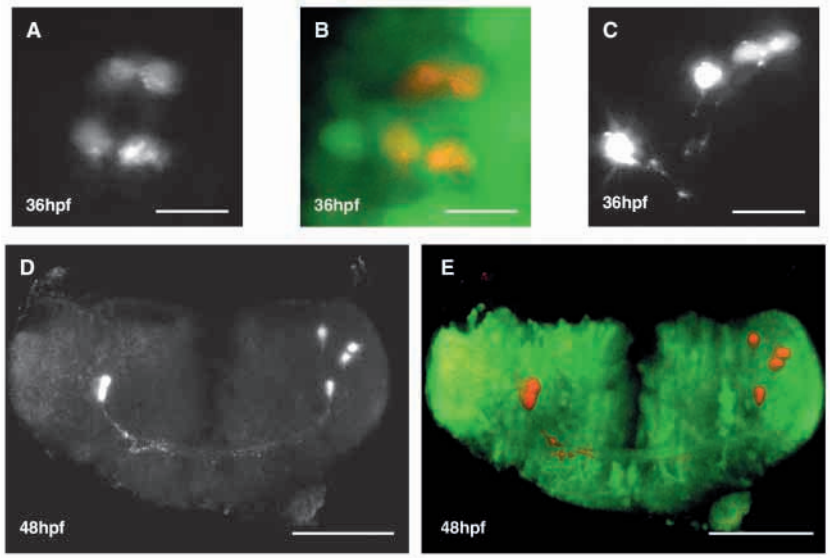

Fig. 3. Neurons can be phenotyped by morphology and/or HuC-GFP expression. (A,B) Dorsal view of four neurons at 36 hpf in the live embryo. Scale bars: 20 μm. (A) Examining the cells by means of dextran visualization alone does not provide conclusive evidence of cell phenotype. (B) Coincidence of dextran-labelled cells with HuC-GFP confirms the cells' phenotype as neuronal. (C) Dorsal view of four neurons at 36 hpf in another live embryo. These four cells can be phenotyped by morphology alone by virtue of their axons. Scale bar: 20 μm. (D) Confocal projection of a clone in a fixed embryo at 48 hpf. Four cells with a neuronal morphology are seen on the right-hand side of the embryonic midline and two cells with a neuronal morphology on the left-hand side. Transverse view with dorsal to the top. Scale bar: 50 μm. (E) Confocal projection of the same specimen as documented in D shows coincident expression of all labelled cells with HuC-GFP. Here we phenotyped cells by morphology and transgene expression. Scale bar: 50 μm.

remaining 11 neurons differentiated directly from the original progenitor without division. Of the 118 neurogenic divisions we observed, only 21% (25/118) generated a progenitor as well as a neuron. In fact, of all progenitor divisions reconstructed, 83% (118/143) generated either two mitotically active progenitor cells or two neurons.

It is possible that the composition of our lineage trees could be influenced by cell death. We have estimated cell death by analysing acridine orange incorporation in rhombomeres 4 and 5. We find an average of 15 dead cells at 15 hpf (n=3), 14 at 24 hpf (n=2), 12 at 36 hpf (n=2) and only 3 at 48 hpf (n=2) in rhombomeres 4 and 5. If clearance of corpses takes an average of 2 hours (Cole and Ross, 2001), then the predicted number of cells undergoing apoptosis between 24 and 36 hours is less than 2% (84/4294) of the total and only 1.3% (72/5367) of the total cells for the period between 36 and 48 hours. Furthermore, the number of cells in our clones never decreased in the intervals between observations and we never detected apoptosis by analysing time-lapse movies of HuC-GFP-positive embryos or Bodipy 505/515-stained embryos between 15 and 36 hpf. These results suggest that cell death plays a minor role in hindbrain development at these stages and suggest that our reconstructed lineage trees are a true representation of clonal development.

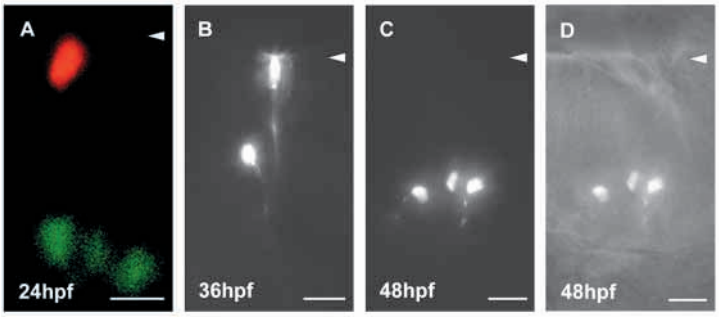

Fig. 4. Direct observation of an asymmetric division. (A) Single cell at 24 hpf labelled with dextran is shown in red. The cell has retracted its process from the pial surface, indicating that it is about to divide at the ventricular surface. Three non-related neurons expressing HuC-GFP are seen at the pial surface. Arrowhead points to ventricular surface. Scale bar: 10 μm. (B-D) Lateral views of the same specimen as in A. Anterior is to the right and dorsal to the top. Arrowheads point to ventricular surface throughout. All scale bars: 20 μm. (B) Two cells are present at 36 hpf following the earlier division. One has a neuronal morphology and one a radial morphology, which may indicate that it is still in the cell cycle. (C) Three neurons with axonal processes are present at 48 hpf, showing that the radial progenitor cell divided again. (D) Same view as C but with brightfield overlay.

Most asymmetric divisions that generate a progenitor and a neuron occur within the plane of the VZ

Previous studies have suggested that the plane of mitosis within the VZ is correlated with the fate of the daughter cells, such that progenitors dividing within the plane of the VZ generate two further progenitors, whereas mitoses that occur perpendicular to the VZ produce an asymmetric division generating one neuron and one progenitor (Chenn and McConnell, 1995). In order to assess this possibility in the zebrafish hindbrain we performed a large-scale analysis of mitotic orientation. We have analysed time-lapse data of progenitors labelled with fluorescent dextran (Fig. 6A-C) and additional material stained with the vital dye Bodipy 505/515 that allows us to visualize cells as they round up in the VZ and divide (Fig. 6D-F). We concentrated on the period between 18-30 hpf because our lineage analysis demonstrated that 28% (19/68) of divisions in this specific period are asymmetric in that they generate both a neuron and a progenitor. However, during this time only 2% (12/557) of progenitor divisions were perpendicular to the plane of the VZ; i.e. divided apico-basally. We conclude that in the zebrafish hindbrain most asymmetric divisions must derive from progenitors that divide in the plane of the VZ.

A small minority of clones still contain progenitors at 48 hpf

Less than 10% of progenitors generated clones that retained putative progenitors at 48 hpf. Seven of the 86 clones fixed

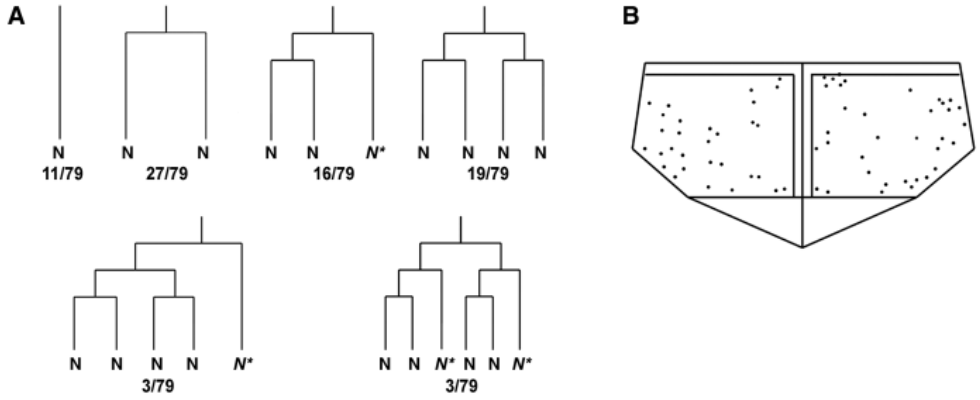

Fig. 5. Summary of lineage trees terminating in neurons only. (A) The composition and frequency of lineage trees observed until 48 hours that produced neurons only. Neurons generated by an asymmetric division are indicated in italics and by an asterisk. (B) Position of 66 neurons taken from clones analysed at 48 hpf projected onto a schematic transverse section through the hindbrain. Neurons are spread over most areas of the mantle layer.

at 48 hpf contained a mixture of neurons and cells with a radial glial morphology. These radial cells had cell bodies within 1-3 cell diameters of the ventricular surface and they did not express GFP in the HuC-GFP embryos (Fig. 7A-C). They often had processes that contacted the ventricular surface and they possessed a single thin process that stretched down towards the pial surface (Fig. 7B,C). At least some of these radial cells will be mitotically active progenitors (see below). Most of these clones (4/7) were composed of two radial cells and two neurons, one clone had two radial cells and three neurons, one had three radial cells and one neuron and the final clone had four radial cells and two neurons. Unfortunately, we were not able to follow the fate of individual cells throughout the development of these clones, therefore we cannot be sure of the precise divisions that generated these neurons and radial cells. However, the two most probable lineage trees for the four clones containing two neurons and two radial cells are shown in Fig. 7D. We have never seen a clone that contained a single radial cell in addition to several neurons.

Radial glia in the fish hindbrain are mitotically active

Although approximately 90% of our lineage trees end with their terminal mitoses before 48 hpf, the hindbrain still has a distinct VZ beyond this time (Fig. 1C,D) and neurogenesis continues at a reduced rate at least up to 72 hpf (Fig. 1F). In order to understand this later neurogenesis we have begun to characterise the cells that comprise the late VZ. First, we have analysed the cell types present in very large clones generated by injecting α-tubulin Gal4UAS-GFP DNA **(**Koster and Fraser 2001) into one-cell stage embryos. The construct is mosaically expressed resulting in large clusters of fluorescent cells and reveals excellent cellular morphology. Cells were classified as neurons if they possessed one or more of the following features: cell body within the HuC-positive domain, and an axon that projects into the marginal zone or ends in a growth cone (Fig. 8A,C). Radial glia were recognised by their cell bodies lying close to the ventricular surface, a short process contacting the ventricle and a radial process stretching to the pial surface (Fig. 8A,B). This analysis revealed that at 48 hpf the hindbrain consists of 91% neurons (233/256) and 9% cells with the morphology of radial glia (23/256).

Radial glia-like processes have previously been described in the zebrafish hindbrain (Trevarrow et al., 1990; Marcus and Easter, 1995) as forming a glial curtain on either side of the rhombomere boundaries. These cells can be revealed by antibodies against GFAP (Nona et al., 1989) and a zebrafish monoclonal antibody, anti-zrf-1 (Trevarrow et al., 1990). Using these antibodies, radial processes are seen to stretch from ventricular to pial surfaces (Fig. 8D,F). In light of recent evidence that radial glia in the rodent cortex are neurogenic progenitors (e.g. Malatesta et al., 2000; Noctor et al., 2001; Noctor et al., 2002), we have investigated whether the radial cells of the zebrafish hindbrain are also progenitors. From approximately 36 hpf we could detect zrf-1 and GFAP immunoreactivity in cell bodies in the VZ. The combination of HuC-GFP and GFAP or zrf-1 immunoreactivity accounted for almost all of the cells of the hindbrain neuroepithelium at these stages. To investigate whether these radial cells divide, we performed double labelling studies with GFAP or zrf-1 and the

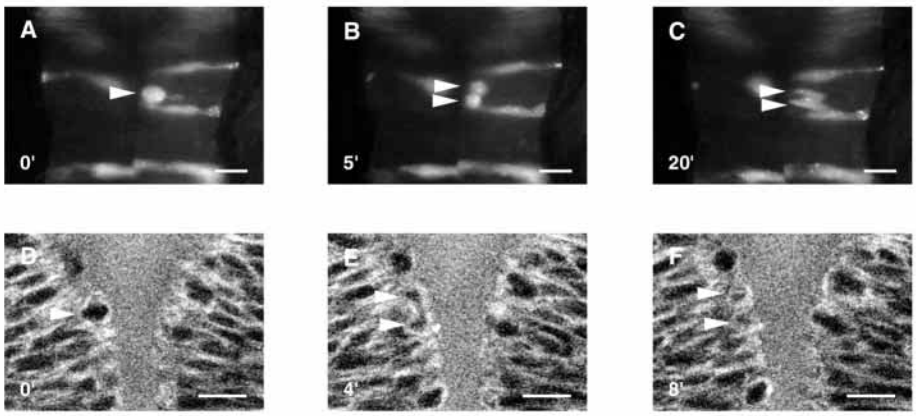

Fig. 6. Orientation of division is almost always within the plane of the ventricular zone. (A-C) Sequence from a time-lapse movie showing a dextran-labelled cell divide along the plane of the ventricular zone. Dorsal view with anterior to the top. Scale bars: 20 μm. (D-E) Sequence from a time-lapse movie illustrating a cell rounding up in the ventricular zone and undergoing mitosis (arrowheads). In this case cells are stained with the vital dye Bodipy 505/515. Dorsal view with anterior to the top. Scale bars: 20 μm.

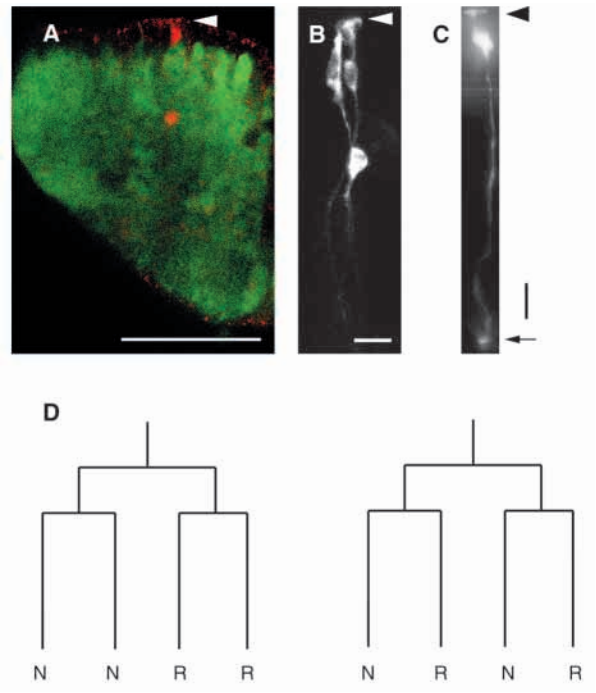

Fig. 7. Non-neuronal cells in clones at 48 hpf. (A) Transverse section through a clone in a HuC-GFP-positive embryo. One cell can be seen near the ventricular surface (arrowhead) outside of the HuC-GFP-positive area. Dorsal is to the top. Scale bar: 50 μm. (B) Lateral view of a clone with three radial cells and a neuron. Arrowhead points to the ventricular zone. Scale bar: 10 μm. (C) Typical morphology of a radial cell at 48 hpf. A distinct endfoot is seen at both the ventricular (arrowhead) and pial (arrow) surfaces. Scale bar: 10 μm. (D) Possible lineage trees for the clones containing two neurons (N) and two radial cells (R).

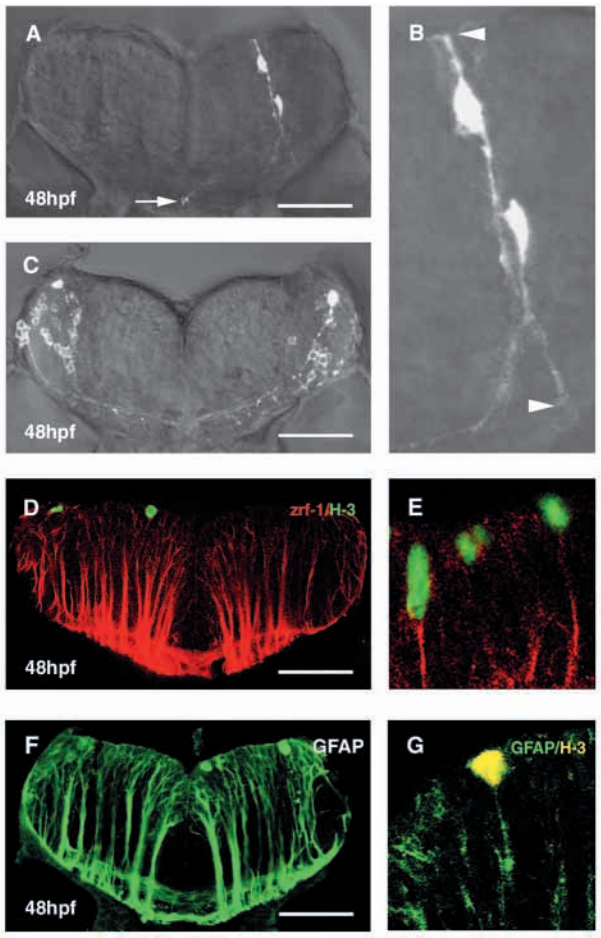

Fig. 8. Neuronal and radial glial cells at 48 hpf. (A) Transverse section at 48 hpf labelled randomly with α-tub Gal4 VP16 UAS GFP. In this specimen we see a single neuron with growth cone (arrowed) and a single cell with a radial glial-like morphology. Scale bar: 50 μm. (B) Higher magnification view of cells seen in A. Arrowheads point to radial glial processes extending to both the ventricular and pial surfaces. (C) Transverse section of hindbrain at the level of rhombomere 5. Confocal projection of neurons labelled at random with α-tub Gal4 VP16 UAS GFP. Scale bar: 50 μm. (D) Confocal section through the hindbrain at 48 hpf double-stained with anti-phosphohistone H-3 (green) and anti-zrf-1 (red). Scale bar: 50 μm. (E) Higher magnification of cells expressing both phosphohistone H-3 and zrf-1. (F) Confocal section through the hindbrain at 48 hpf stained with anti-GFAP (green). Scale bar: 50 μm. (G) High magnification of a single cell expressing both phosphohistone H-3 (yellow) and anti-GFAP (green).

mitotic marker phosphohistone H-3 (H-3) (Juan et al., 1998). Many of the GFAP/zrf-1-positive cells also expressed H-3 (Fig. 8E,G). These data demonstrate that at 48 hpf the zebrafish hindbrain is composed largely of neurons and cells with radial glial morphology and that some of these radial cells are mitotically active progenitors.

DISCUSSION

By following the fate of fluorescently labelled neural progenitors through to their terminal divisions, we have determined that the majority of neurons in the zebrafish embryo hindbrain are born from progenitor divisions that generate two neurons. Divisions that generate a progenitor as well as a neuron do occur, but they represent only 17% of the progenitor divisions monitored and many of these asymmetric divisions appear to be restricted to a particular generation within a family tree. More than 90% of the progenitors monitored from the neural rod stage had their terminal mitoses prior to 48 hpf. Our results show that in the embryonic zebrafish hindbrain most progenitors do not follow a stem cell mode of division. These results represent the first direct observations and quantification of neurogenic divisions in an intact vertebrate nervous system.

Probabilities and implications for mechanisms

We wanted to be confident that our lineage tree analysis could account quantitatively for neurogenesis in the zebrafish hindbrain. The 86 original progenitors in our lineage analysis produce a total of 236 neurons by 48 hpf. This gives a factor of 2.74 neurons produced per progenitor. This data predicts that the 1618 progenitor cells actually present in rhombomeres 4 and 5 at 15 hpf should generate 2.74×1618 (4440) neurons by 48 hpf. In fact, our cell counts reveal that there are 4150 HuC-GFP-positive cells present at 48 hpf. This confirmed that the lineage data predicts actual neurogenesis with an error of only 7%.

We have quantified progenitor divisions according to whether they generate progenitors, neurons or a combination of the two. Table 1 shows the relative proportion of each of these division modes at the first and second rounds of division in our lineage analysis, and Table 2 shows the percentage of neurons and non-neuronal cells generated at each division. After the first division there seems to be an almost equal probability that an individual cell will differentiate into a neuron (54%) or re-enter the cell cycle (46%) (Table 2). However, there is also a strong bias towards divisions that generate either two neurons (40%) or two progenitors (32%) with progenitor/neuron divisions occurring at a frequency well below that predicted by chance alone (Table 1). After the second division there is an overwhelming bias for daughter cells to differentiate as neurons (90%) and a consequent strong bias for both daughter cells to be neurons (86%). Our data shows that the vast majority of neurons generated throughout hindbrain neurogenesis are born via a terminal neurogenic division. Thus for the majority of hindbrain neurons the mechanism that commits cells to a neuronal fate is not linked to a mechanism that determines asymmetric division. The strategy of using symmetric divisions to first expand the progenitor population and then to generate pairs of neurons through terminal divisions is the quickest mechanism to generate many neurons in a small number of rounds of division. Thus only two rounds of division are needed for each progenitor to generate four neurons. A progenitor that divides in an asymmetric stem cell mode would require four rounds of division to make the same number of neurons. The majority of hindbrain progenitors thus appear to behave like 'transit amplifying cells' rather than stem cells. Transit amplifying cells have previously been described in both neural and non-neural progenitor pools where they characteristically undergo a limited number of rounds of division before terminally differentiating (Doetsch et al., 2002; Potten and Loeffler, 1990).

It is obviously important that some progenitors are maintained beyond 48 hpf for later neurogenesis and gliogenesis. In the zebrafish hindbrain it appears that as few as 10% of the original progenitor population are retained for these later events. Whether this 10% of progenitors arises randomly from the original population or whether they are determined early and set aside by specific mechanisms remains an important issue to address in the future.

Signalling via the Notch pathway has been shown to be an important mechanism that restricts the premature differentiation of cells in the zebrafish neural plate and neural tube (Haddon et al., 1998; Gray et al., 2001; Itoh et al., 2003). Loss of Notch-Delta signalling in the zebrafish *mind bomb* mutant leads to a spinal cord apparently depleted of progenitors and composed entirely of neurons by 24 hpf (Itoh et al., 2003). Our own observations suggest that although the *mind bomb* hindbrain is also largely composed of prematurely differentiating neurons, a small population of progenitors remain even at 60 hpf, perhaps suggesting some progenitors are maintained by mechanisms other than the Notch-Delta pathway (D.A.L. and J.D.W.C., unpublished).

Table 1. Frequency of phenotypes in daughter cell pairs derived from the first and second rounds of division

	Neuron+ neuron	Progenitor+ progenitor	Neuron+ progenitor
First division	40% (22/68)	32% (27/68)	28% (19/68)
Second division	86% (54/63)	5% (3/63)	9% (6/63)

Table 2. Overall frequency of neuronal and progenitor cells derived from the first and second rounds of division

	Neurons	Progenitors
First division	54% (73/136)	46% (63/136)
Second division	90% (114/126)	10% (12/126)

Asymmetric divisions in other vertebrate systems

Our results demonstrate that progenitors exhibiting asymmetric stem cell-like behaviour are rare during the major phase of embryonic hindbrain neurogenesis. However, both birth-dating studies and clonal analyses (e.g. Takahashi et al., 1996; Mione et al., 1997; Cai et al., 2002) suggest that asymmetric stem cell divisions do occur in the mammalian cortex, but direct evidence for divisions that generate one progenitor and one post-mitotic cell in the intact brain is scarce. Evidence has recently been provided from cortical slice preparations that radial glia, infected with retroviruses expressing GFP and followed by time-lapse microscopy, can divide (Noctor et al., 2001). Clonal analysis in this study revealed individual radial glial progenitors alongside neurons at varying times after infection, suggesting that they divided asymmetrically to generate the neurons (Noctor et al., 2001). In vitro studies (Qian et al., 1998; Shen et al., 2002) have followed cells isolated from embryonic mouse cortex between E10.5 and E13 and monitored their behaviour using video time-lapse microscopy. In a minority of clones analysed a stereotyped asymmetric division is described in which one daughter cell divides once more to generate two neurons whereas the other daughter divided more than once more. In this case the asymmetric divisions produces two progenitors with different fates (Qian et al., 1998) as is the case for the division of the *Drosophila* neuroblast. In fact, the majority of clones followed in this in vitro study expanded by divisions that generated either two progenitors or two differentiated progeny (Qian et al., 1998). In a more recent in vitro study from the same lab, some divisions generated both a progenitor and a neuron under similar culture conditions (Shen et al., 2002). The precise behaviour of these progenitors in vivo remains to be determined.

Correlation between cell fate and plane of division

Initial reports claimed cortical progenitors dividing within the plane of the VZ generated daughter cells that adopted symmetrical fates, whereas progenitors dividing perpendicular to the plane of the VZ generated daughters with asymmetric fates (Chenn and McConnell, 1995). This study reported that the cell that left the VZ expressed notch 1 asymmetrically with respect to its sister. However, the fate of these cells was never followed for a sufficiently long period to determine their phenotype unequivocally. Recently, others have readdressed this question and conflicting reports have been published (Cayouette et al., 2001; Silva et al., 2002; Das et al., 2003). In one study the authors demonstrate that in the rat retina the proportion of cells dividing out of the plane of the VZ peaks at P0 at 21%. The daughter cells of these divisions are shown

to inherit Numb protein asymmetrically. However, these observations are made long after the bulk of retinal neurons have been generated and do not address the fate of the daughter cells (Cayouette et al., 2001). In a chick retinal study the orientation of division was compared between regions where neurons were being produced and regions where neurons were not being produced. In this study no difference in the orientation of division between these two regions is reported (Silva et al., 2002). In a more recent study in the zebrafish retina, a change in the orientation of division between the central-peripheral to circumferential axes was reported to coincide with the onset of neurogenesis but no cells were seen to divide out of the plane of the VZ (Das et al., 2003). It is suggested that this change in orientation is linked to the switch from proliferative to neurogenic divisions. However, no evidence is provided that asymmetric cell fate occurs in any of these studies, so a correlation between fate, division mode and orientation cannot be made. Our study addresses this issue more directly because our analysis of division orientation is made during a period when we have demonstrated a relatively high proportion of asymmetrically fated divisions. Our findings do not agree with the original Chenn and McConnell model of apico-basal asymmetric divisions, and strongly suggest that asymmetrically fated divisions usually occur in the plane of the VZ.

Radial glia and late progenitors

Trevarrow et al. (Trevarrow et al., 1990) described the stereotyped arrangement of many cell types within a zebrafish rhombomere. One cell type formed a glial curtain of radial processes on either side of the rhombomere boundaries. We have characterised these cells further and found that their cell bodies are located in the VZ in an area devoid of HuC-GFP expression and that they have a distinct radial glial morphology. Importantly, we find that many of these cells express both glial and mitotic markers. We conclude that at least a subset of these radial glial cells are progenitor cells. Other studies have demonstrated similar functions for radial glia in the mammalian forebrain (Hartfuss et al., 2001; Malatesta et al., 2000; Miyata et al., 2001; Noctor et al., 2001; Noctor et al., 2002; Tamamaki et al., 2001; Heins et al., 2002). It is probable that radial glia are a heterogeneous population with subsets expressing distinct molecular profiles and that this may reflect differences in their behavioural phenotype (Hartfuss et al., 2001). We have direct evidence that some radial cells of the glial curtain are neurogenic progenitors (A.T.G. and J.D.W.C., unpublished) and it is probable that other subsets will give rise to oligodendrocyte precursors and mature astroglial cells.

We have focused our analysis on progenitor divisions that generate neurons and for this purpose we defined an asymmetric division as one that generates both a neuron and a progenitor. In the strict sense it is possible that divisions that generate two progenitors or two neurons may also be asymmetric if the daughter cells are intrinsically different to one another, but we have not analysed this possibility here. The *Drosophila* neuroblast divides asymmetrically to produce another neuroblast and a ganglion mother cell, which is itself another progenitor but with a more limited potential (reviewed by Lu et al., 2000). Also in the fly, asymmetric divisions have been shown to generate two different types of neuron (Bossing et al., 1996), thus helping to generate the diversity of differentiated cells. In the vertebrate brain, neuronal diversity is thought to be largely generated by extrinsic signals acting on neuronal progenitors (Edlund and Jessell, 1999) rather than through the mechanisms of asymmetric division. In line with this, single hindbrain progenitors in the chick embryo tend to generate clones of neurons of a restricted subclass (Lumsden et al., 1994), and the identity of the neurons generated in these clones is correlated with the position that the progenitors occupy in the dorsoventral axis (Clarke et al., 1998). In the future we intend to address the issue of neuronal phenotypes in our zebrafish clones to determine whether there are any consistent asymmetries in the identity of sibling neurons, but for the moment our analysis has centred on the decision of whether to make a neuron or not. Our study has of course only described the fate of daughter cells rather than their potential. We do not know that the daughter cells fated to become neurons were determined at or before their terminal mitosis or that the determining step occurred simultaneously in both daughters (but our unpublished evidence shows that the time between neuronal birth and HuC-GFP expression is very stereotyped in post-mitotic neurons). However, it is possible that there could be an asymmetry in sibling potential that is not apparent from simply monitoring their fate. This will be an important issue to address in the future.

In conclusion, our work has provided the first in vivo analysis of neurogenesis at the level of both the individual cell and the population as a whole in a vertebrate. Our results suggest that in this vertebrate system the molecular determinants that control whether a cell will become a neuron are usually not linked to a mechanism that generates asymmetric divisions. We believe that this analysis has provided key insights into how the majority of embryonic neurons are generated in a vertebrate system and provides a good framework against which genetic manipulations can be targeted in the future.

We thank Philippa Bayley, Marcel Tawk, Steve Wilson and Lewis Wolpert for helpful comments on the manuscript. The work was funded by the Anatomy Department UCL, the BBSRC and the Wellcome Trust.

REFERENCES

Bossing, T., Udolph, G., Doe, C. Q. and Technau, G. M. (1996). The embryonic central nervous system lineages of *Drosophila melanogaster*. I. Neuroblast lineages derived from the ventral half of the neuroectoderm. *Dev. Biol.* **179**, 41-64.

Brewster, R. and Bodmer, R. (1996). Cell lineage analysis of the *Drosophila* peripheral nervous system. *Dev. Genet.* **18**, 50-63.

Cai, L., Hayes, N. L., Takahashi, T., Caviness, V. S., Jr and Nowakowski, R. S. (2002). Size distribution of retrovirally marked lineages matches prediction from population measurements of cell cycle behavior. *J. Neurosci. Res.* **69**, 731-744.

Cayouette, M., Whitmore, A. V., Jeffery, G. and Raff, M. (2001). Asymmetric segregation of Numb in retinal development and the influence of the pigmented epithelium. *J. Neurosci.* **21**, 5643-5651.

Chenn, A. and McConnell, S. K. (1995). Cleavage orientation and the asymmetric inheritance of Notch1 immunoreactivity in mammalian neurogenesis. *Cell* **82**, 631-641.

Clarke, J. D. (1999). Using fluorescent dyes for fate mapping, lineage analysis, and axon tracing in the chick embryo. *Methods Mol. Biol.* **97**, 319-328.

Clarke, J. D., Erskine, L. and Lumsden, A. (1998). Differential progenitor

dispersal and the spatial origin of early neurons can explain the predominance of single-phenotype clones in the chick hindbrain. *Dev. Dyn.* **212**, 14-26.

Cole, L. K. and Ross, L. S. (2001). Apoptosis in the developing zebrafish embryo. *Dev. Biol.* **240**, 123-142.

Das, T., Payer, B., Cayouette, M. and Harris, W. A. (2003). In vivo time-lapse imaging of cell divisions during neurogenesis in the developing zebrafish retina. *Neuron* **37**, 597-609.

Doetsch, F., Petreanu, L., Caille, I., Garcia-Verdugo, J. M. and Alvarez-Buylla, A. (2002). EGF converts transit-amplifying neurogenic precursors in the adult brain into multipotent stem cells. *Neuron* **36**, 1021-1034.

Edlund, T. and Jessell, T. M. (1999). Progression from extrinsic to intrinsic signaling in cell fate specification: a view from the nervous system. *Cell* **96**, 211-224.

Fraser, S., Keynes, R. and Lumsden, A. (1990). Segmentation in the chick embryo hindbrain is defined by cell lineage restrictions. *Nature* **344**, 431-435.

Gray, M., Moens, C. B., Amacher, S. L., Eisen, J. S. and Beattie, C. E. (2001). Zebrafish deadly seven functions in neurogenesis. *Dev. Biol.* **237**, 306-323.

Haddon, C., Smithers, L., Schneider-Maunoury, S., Coche, T., Henrique, D. and Lewis, J. (1998). Multiple delta genes and lateral inhibition in zebrafish primary neurogenesis. *Development* **125**, 359-370.

Hartfuss, E., Galli, R., Heins, N. and Gotz, M. (2001). Characterization of CNS precursor subtypes and radial glia. *Dev. Biol.* **229**, 15-30.

Heins, N., Malatesta, P., Cecconi, F., Nakafuku, M., Tucker, K. L., Hack, M. A., Chapouton, P., Barde, Y. A. and Gotz, M. (2002). Glial cells generate neurons: the role of the transcription factor Pax6. *Nat. Neurosci.* **5**, 308-315.

Hirata, J., Nakagoshi, H., Nabeshima, Y. and Matsuzaki, F. (1995). Asymmetric segregation of the homeodomain protein Prospero during *Drosophila* development. *Nature* **377**, 627-630.

Itoh, M., Kim, C. H., Palardy, G., Oda, T., Jiang, Y. J., Maust, D., Yeo, S. Y., Lorick, K., Wright, G. J., Ariza-McNaughton, L. et al. (2003). Mind bomb is a ubiquitin ligase that is essential for efficient activation of notch signaling by delta. *Dev. Cell* **4**, 67-82.

Juan, G., Traganos, F., James, W. M., Ray, J. M., Roberge, M., Sauve, D. M., Anderson, H. and Darzynkiewicz, Z. (1998). Histone H3 phosphorylation and expression of cyclins A and B1 measured in individual cells during their progression through G2 and mitosis. *Cytometry* **32**, 71-77.

Kimmel, C. B., Warga, R. M. and Kane, D. A. (1994). Cell cycles and clonal strings during formation of the zebrafish central nervous system. *Development* **120**, 265-276.

Kimmel, C. B., Ballard, W. W., Kimmel, S. R., Ullmann, B. and Schilling, T. F. (1995). Stages of embryonic development of the zebrafish. *Dev. Dyn.* **203**, 253-310.

Kornack, D. R. and Rakic, P. (1995). Radial and horizontal deployment of clonally related cells in the primate neocortex: relationship to distinct mitotic lineages. *Neuron* **15**, 311-321.

Koster, R. W. and Fraser, S. E. (2001). Tracing transgene expression in living zebrafish embryos. *Dev. Biol.* **233**, 329-346.

Kubu, C. J., Orimoto, K., Morrison, S. J., Weinmaster, G., Anderson, D. J. and Verdi, J. M. (2002). Developmental changes in Notch1 and numb expression mediated by local cell-cell interactions underlie progressively increasing delta sensitivity in neural crest stem cells. *Dev. Biol.* **244**, 199-214.

Lu, B., Jan, L. and Jan, Y. N. (2000). Control of cell divisions in the nervous system: symmetry and asymmetry. *Annu. Rev. Neurosci.* **23**, 531-556.

Lumsden, A., Clarke, J. D., Keynes, R. and Fraser, S. (1994). Early phenotypic choices by neuronal precursors, revealed by clonal analysis of the chick embryo hindbrain. *Development* **120**, 1581-1589.

Malatesta, P., Hartfuss, E. and Gotz, M. (2000). Isolation of radial glial cells by fluorescent-activated cell sorting reveals a neuronal lineage. *Development* **127**, 5253-5263.

Marcus, R. C. and Easter, S. S., Jr (1995). Expression of glial fibrillary acidic protein and its relation to tract formation in embryonic zebrafish (Danio rerio). *J. Comp. Neurol.* **359**, 365-381.

Mione, M. C., Cavanagh, J. F., Harris, B. and Parnavelas, J. G. (1997). Cell fate specification and symmetrical/asymmetrical divisions in the developing cerebral cortex. *J. Neurosci.* **17**, 2018-2029.

Miyata, T., Kawaguchi, A., Okano, H. and Ogawa, M. (2001). Asymmetric inheritance of radial glial fibers by cortical neurons. *Neuron* **31**, 727-741.

Noctor, S. C., Flint, A. C., Weissman, T. A., Dammerman, R. S. and Kriegstein, A. R. (2001). Neurons derived from radial glial cells establish radial units in neocortex. *Nature* **409**, 714-720.

Noctor, S. C., Flint, A. C., Weissman, T. A., Wong, W. S., Clinton, B. K. and Kriegstein, A. R. (2002). Dividing precursor cells of the embryonic cortical ventricular zone have morphological and molecular characteristics of radial glia. *J. Neurosci.* **22**, 3161-3173.

Nona, S. N., Shehab, S. A., Stafford, C. A. and Cronly-Dillon, J. R. (1989). Glial fibrillary acidic protein (GFAP) from goldfish: its localisation in visual pathway. *Glia* **2**, 189-200.

Park, H. C., Hong, S. K., Kim, H. S., Kim, S. H., Yoon, E. J., Kim, C. H., Miki, N. and Huh, T. L. (2000a). Structural comparison of zebrafish Elav/Hu and their differential expressions during neurogenesis. *Neurosci. Lett.* **279**, 81-84.

Park, H. C., Kim, C. H., Bae, Y. K., Yeo, S. Y., Kim, S. H., Hong, S. K., Shin, J., Yoo, K. W., Hibi, M. and Hirano, T. et al. (2000b). Analysis of upstream elements in the HuC promoter leads to the establishment of transgenic zebrafish with fluorescent neurons. *Dev. Biol.* **227**, 279-293.

Petersen, P. H., Zou, K., Hwang, J. K., Jan, Y. N. and Zhong, W. (2002). Progenitor cell maintenance requires *numb* and *numblike* during mouse neurogenesis. *Nature* **419**, 929-934.

Potten, C. S. and Loeffler, M. (1990). Stem cells: attributes, cycles, spirals, pitfalls and uncertainties. Lessons for and from the crypt. *Development* **110**, 1001-1020.

Qian, X., Goderie, S. K., Shen, Q., Stern, J. H. and Temple, S. (1998). Intrinsic programs of patterned cell lineages in isolated vertebrate CNS ventricular zone cells. *Development* **125**, 3143-3152.

Qian, X., Shen, Q., Goderie, S. K., He, W., Capela, A., Davis, A. A. and Temple, S. (2000). Timing of CNS cell generation: a programmed sequence of neuron and glial cell production from isolated murine cortical stem cells. *Neuron* **28**, 69-80.

Shankland, M. (1995). Formation and specification of neurons during the development of the leech central nervous system. *J. Neurobiol.* **27**, 294-309.

Shen, Q., Zhong, W., Jan, Y. N. and Temple, S. (2002). Asymmetric Numb distribution is critical for asymmetric cell division of mouse cerebral cortical stem cells and neuroblasts. *Development* **129**, 4843-4853.

Silva, A. O., Ercole, C. E. and McLoon, S. C. (2002). Plane of cell cleavage and *numb* distribution during cell division relative to cell differentiation in the developing retina. *J. Neurosci.* **22**, 7518-7525.

Skeath, J. B. and Doe, C. Q. (1996). The achaete-scute complex proneural genes contribute to neural precursor specification in the *Drosophila* CNS. *Curr. Biol.* **6**, 1146-1152.

Sterio, D. C. (1984). The unbiased estimation of number and sizes of arbitrary particles using the disector. *J. Microsc.* **134**, 127-136.

Takahashi, T., Nowakowski, R. S. and Caviness, V. S., Jr (1996). The leaving or Q fraction of the murine cerebral proliferative epithelium: a general model of neocortical neuronogenesis. *J. Neurosci.* **16**, 6183-6196.

Tamamaki, N., Nakamura, K., Okamoto, K. and Kaneko, T. (2001). Radial glia is a progenitor of neocortical neurons in the developing cerebral cortex. *Neurosci. Res.* **41**, 51-60.

Trevarrow, B., Marks, D. L. and Kimmel, C. B. (1990). Organization of hindbrain segments in the zebrafish embryo. *Neuron* **4**, 669-679.

Verdi, J. M., Bashirullah, A., Goldhawk, D. E., Kubu, C. J., Jamali, M., Meakin, S. O. and Lipshitz, H. D. (1999). Distinct human NUMB isoforms regulate differentiation vs. proliferation in the neuronal lineage. *Proc. Natl. Acad. Sci. USA* **96**, 10472-10476.

Wakamatsu, Y., Maynard, T. M., Jones, S. U. and Weston, J. A. (1999). NUMB localizes in the basal cortex of mitotic avian neuroepithelial cells and modulates neuronal differentiation by binding to NOTCH-1. *Neuron* **23**, 71-81.

Wakamatsu, Y., Maynard, T. M. and Weston, J. A. (2000). Fate determination of neural crest cells by NOTCH-mediated lateral inhibition and asymmetrical cell division during gangliogenesis. *Development* **127**, 2811-2821.

Zhong, W., Jiang, M. M., Weinmaster, G., Jan, L. Y. and Jan, Y. N. (1997). Differential expression of mammalian Numb, Numblike and Notch1 suggests distinct roles during mouse cortical neurogenesis. *Development* **124**, 1887-1897.

Zhong, W., Jiang, M. M., Schonemann, M. D., Meneses, J. J., Pedersen, R. A., Jan, L. Y. and Jan, Y. N. (2000). Mouse *numb* is an essential gene involved in cortical neurogenesis. *Proc. Natl. Acad. Sci. USA* **97**, 6844-6849.

Zilian, O., Saner, C., Hagedorn, L., Lee, H. Y., Sauberli, E., Suter, U., Sommer, L. and Aguet, M. (2001). Multiple roles of mouse Numb in tuning developmental cell fates. *Curr. Biol.* **11**, 494-501.